POAC'15
Trondheim, Norway

Proceedings of the 23rd International Conference on
Port and Ocean Engineering under Arctic Conditions
June 14-18, 2015
Trondheim, Norway

STRUCTURAL RESPONSE COMPARISON USING DIFFERENT APPROACHES TO ACCOUNT FOR ICE LOADING

Boris Erceg [1], Rocky Taylor [2], Sören Ehlers [1, 3]
[1]Norwegian University of Science and Technology, Trondheim, Norway
[2] Memorial University of Newfoundland, St. John's, NL, Canada
[3] Hamburg University of Technology, Hamburg, Germany

ABSTRACT
Ships operating in ice-covered waters need to comply with the route-specific ice-induced loads. Compliance with classification societies' rules is achieved through the introduction of a uniform pressure patch applied to the hull surface. As this approach aims to capture the average force acting over the specified panel area, it does not directly account for the high degree of spatial and temporal variations observed in ice load measurements, which are inherent to the ice failure process. Furthermore, the current formulations of ice class rules do not fully account for the probabilistic nature of ice loads, i.e. scale effects for local ice pressures captured in full-scale measurements. Finally, ice class rules do not consider route-specific ice conditions when estimating the design load, i.e. the exposure of the vessel to ice crushing as determined by the number and duration of rams.
The current paper addresses those discrepancies, previously studied by Erceg et al. (2014, 2015), through the response comparison of a stiffened panel subjected to ice loads using different approaches to account for ice loading.
Full-scale pressure distributions obtained from Japanese Ocean Industries Association (JOIA) field indentation programme are used to investigate the effects of spatially localized loads on the local plastic deformation of the hull. The results obtained using the Finite Element Method (FEM) are compared to the rule-based method as well as the rational approach for design load estimation developed by Jordaan and co-workers.

INTRODUCTION
Global trends in hydrocarbon exploration together with the reductions in the severity of ice conditions have increased the number of ships operating in the arctic region. Ships sailing in those ice-covered waters experience intense loads from ice features, particularly multi-year ice. Thus, in order to prevent ice-induced damages (Kujala, 1991) and ensure safe and economically sound operations, structural design, i.e. selection of an appropriate ice class, is paramount. Kujala & Ehlers (2013, 2014) addressed the latter through a risk-based assessment of the required level of ice strengthening in view of life-cycle costs and eventual repair costs.

Ships sailing in first-year ice environments are usually designed according to the Finnish-Swedish Ice Class Rules (FSICR), the oldest set of regulations for the design of ice-going vessels. Although primarily intended for the Baltic Sea navigation, decades of experience including numerous damage surveys and full-scale measurements propelled the FSICR to the status of an "industry standard" for ships sailing in first-year ice environments. Thus, they are

incorporated in the rules of most major classification societies. For more details and background on the FSICR, reader is referred to Trafi (2010) and Riska & Kämäräinen (2011).

Ice-induced loads are known to have a strong stochastic behaviour due to the stochastic nature of ice properties and the "chaotic" ship-ice interaction process. As ice is formed in nature, numerous parameters affect its mechanical and physical properties. Furthermore, ship operations in ice have various forms (e.g. icebreakers' assistance, independent navigation) with inclusion of different ice features. Finally, the icebreaking process and load carrying mechanisms under ice loads are not fully understood yet.

Regarding hull structural design, there are discrepancies in the way ice loads are treated in the rule-based design approach and the nature of loads measured in field tests. Given a highly stochastic nature of the ice properties, ice loads exert high spatial and temporal variations as a result of the ice failure; see e.g. Jordaan (2001), Erceg et al. (2014), Richard & Taylor (2014), Taylor & Richard (2014). Instead, the FSICR suggest reaching compliance with their requirements by introducing a rectangular uniform pressure patch on the hull surface. Additionally, they apply general safety margins for different structural elements, in spite of the fact that different types of ice loading alter the stress distribution and therefore change the response of the structure. Furthermore, the FSICR do not consider route-specific ice conditions in determining the design load, i.e. the exposure of the vessel to ice crushing determined by the number and duration of loading events. Erceg et al. (2014) analysed medium-scale ice crushing indentation tests and subjected a stiffened panel to the measured load pattern. They concluded that the utilization of long-term maximum loads from the ship-ice interaction measurements does not resemble the important phenomena, such as spatial and temporal variations, sufficiently when converted into a uniform pressure patch.

Jordaan et al. (1993) developed an approach for the design of arctic ships based on probabilistic methods. The approach includes global impact forces and local panel design, combining seasonal and regional variability in environmental conditions with uncertainty, i.e. the probability of exceedence. The design curve therein is given as

$$\alpha = 1.25a^{-0.7} \tag{1}$$

where a is the local design area (m^2) and is and α is a constant for a given area (MPa). The equation is based on the Kigoriak ship ram trial dataset, which represents the highest pressures amongst the available ship-ice interaction data. It thus serves as an appropriate upper bound for local ice pressure estimations. Local panel design therein starts off with the assessment of global interaction processes based on full-scale measurements or numerical interaction models in order to obtain the parent distribution of impact forces. This single event distribution is then used to obtain the local design load by accounting for the vessel's exposure to ice crushing. Exposure is a key input for local design analysis, and is determined by the number and duration of interaction events, as well as by the proportion of hits on the selected area relative to those on the overall structure. For more details on the method see Taylor et al. (2009) and Ralph & Jordaan (2013).

Erceg et al. (2015) used the probabilistic approach based on the measured data and expected exposure so as to select an appropriate ice class for a vessel navigating along the Northern Sea Route. The design pressures and the response of the structure by means of von Mises stress were compared to those obtained by using the rule-based design approach. The FE-analysis showed significantly higher stress levels when using the probabilistic approach, followed by plastic deformations of the structure. The latter clearly identified the need for an alternative

design approach that would include important ice phenomena, such as line-like load and high-pressure zones (*hpz*s).

This paper continues the work published in Erceg et al. (2014, 2015) and compares the structural response of a stiffened panel to ice loads using two different design approaches (rule-based design method and probabilistic method for the design of arctic ships) to full-scale pressure distributions captured in the field measurements. The logic behind each approach is briefly described in the paper and the methodology is backed up with an illustrative example. The response analyses are performed by means of FE-simulations using the explicit solver LS-DYNA and ANSYS parametric design language. The resulting compliance of the design load and response for the chosen structure is presented and discussed.

DESIGN APPROACHES

Rule-based method

The current version of the FSCIR (Trafi, 2010) includes requirements for hull, machinery, and minimum propulsion power. The strength level of four available ice classes (IA Super, IA, IB, IC) corresponds roughly to the loading from a certain level of ice thickness. The ice class factor is represented by the height of the loading area, which is taken as a fraction of ice thickness; e.g., ice class IAS corresponds to the loading of approx. 1 m thick level ice, whereas the loading height is taken as 0.35 m. The design requirement is a collision with the ice channel edge at the minimum speed of 5 knots, where yield is the design limit state. The definition of ice pressure and ice loads is an integral part of the hull rules. Design pressure is defined as:

$$p = c_d \cdot c_p \cdot c_a \cdot p_0 \tag{2}$$

where p_0 is the nominal ice pressure and is taken to be constant (5.6 MPa) for all ice classes, as the ice properties across the Baltic Sea do not change significantly during an average winter. Displacement and engine power of the ship are taken into account through the factor c_d, while c_p adjusts the design pressure in accordance to the hull region (bow, mid-body, stern) where the load occurs. Finally, factor c_a is dependent on the characteristic load length that influences the response in a particular structural member; see Table 4. Consequently, four design pressures corresponding to different structural elements are obtained and used to calculate their respective scantlings.

When conducting direct analyses, Trafi (2010) suggests the load patch to be applied at locations where the capacity of the structure under combined effects of bending and shear is minimized. That includes several vertical locations in between upper and lower ice waterlines and several horizontal locations, especially those centred at the mid-span or -spacing. The response of the different structural members shall be checked for pressure patch areas defined by load lengths, l_a, given in Table 1 and the loading height specified in the FSICR. Trafi (2010) states that "the acceptance criterion for designs is that the combined stresses from bending and shear, using the von Mises yield criterion, are lower than the yield point of the material, σ_y", which is consistent to the analysis of Riska & Kämäräinen (2011). Figure 1 shows an example of loading cases for structural analysis of a stiffened panel in the ice belt region.

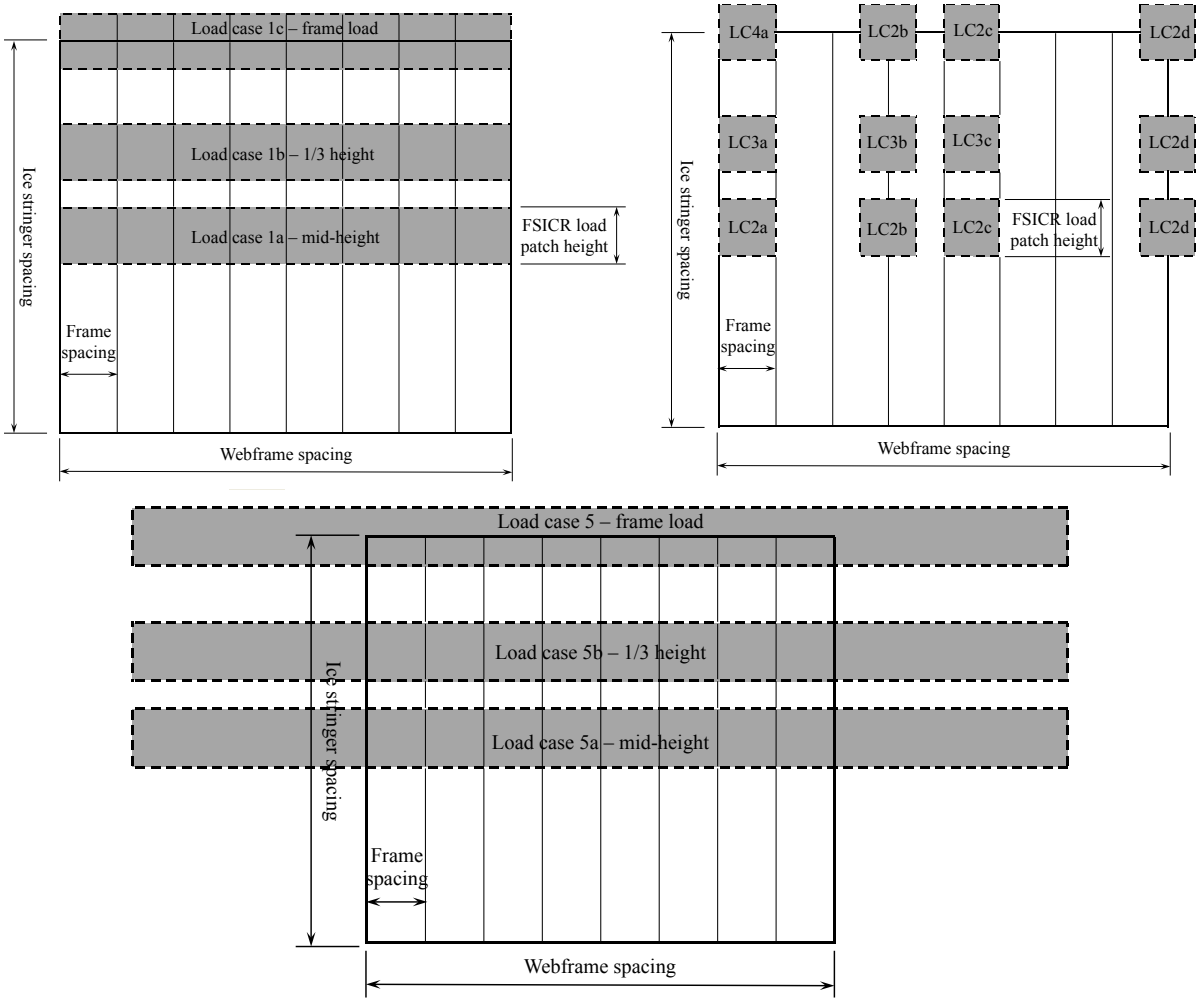

Figure 1. Example of loading cases for structural analysis of a stiffened panel in the ice belt region (as defined in Trafi, 2010).

Probabilistic method

For the local structural design, a global ram analysis is first carried out from which an average ram duration and penetration are determined. Local pressures on individual panel areas are modelled using an exponential distribution for peak panel pressures given as:

$$F_x(x) = 1 - \exp\left(-\frac{x - x_0}{\alpha}\right) \tag{3}$$

where x_0 is the panel exposure constant and x is a random quantity denoting pressure. The number of events can be modelled as a Poisson process to give the peak local pressure distribution as

$$F_z(z) = \exp\left\{-\exp\left(\frac{z - x_0 - x_1}{\alpha}\right)\right\} \tag{4}$$

where $x_1=\alpha(\ln\mu)$ and μ is the design exposure, modelled as the proportion of events that represent actual panel hits given as

$$\mu = v \cdot r \cdot \frac{t}{t_k} \tag{5}$$

This accounts for the expected number of impacts in a time period, v, proportion of events giving "direct hits" on a specified panel, r, and the duration of impact events, t. Parameter t_k is the reference duration associated with the design curve from Jordan et al. (1993). Finally, the design load, z_e, corresponding to a given exceedence probability $F_z(z_e)$, can be determined as

$$z_e = x_0 + \alpha\left\{-\ln\left[-\ln F_z(z_e)\right] + \ln \mu\right\} \qquad (6)$$

Figure 2 shows the results for α versus area curves for each dataset analysed by Taylor et al. (2009), in addition to the bounding curve from Eq. (1). A series of best-fit curves of the form $\alpha = Ca^D$ were fitted to each dataset to allow comparison with the design curve, where parameters C and D are constants corresponding to each dataset. Furthermore, the figure shows that the pressures follow a decreasing trend with increasing area, which suggests the dependency on some physical characteristic of the interaction, such as the ice type, thickness or temperature. Coefficient C appears to be most influenced by the ice type, where thicker and stronger ice has higher C values, while thinner first-year events where flexural failure may be more dominant have smaller values and result in lower pressures. The exponent D was observed to range from -0.8 to -0.6 with a mean value of -0.7. The values are consistent both for first-year and multi-year ice datasets. Therefore, for design in multi-year ice environments it is reasonable to use the bounding curve as a conservative assumption. For first-year ice environments, however, the design equation overestimates the local pressures by a considerable margin and the use of design equations corresponding to the datasets under ice loading conditions similar to those expected for the design environment may be more appropriate. The reader is referred to Taylor et al. (2009) for a complete discussion on analysed ship-interaction data.

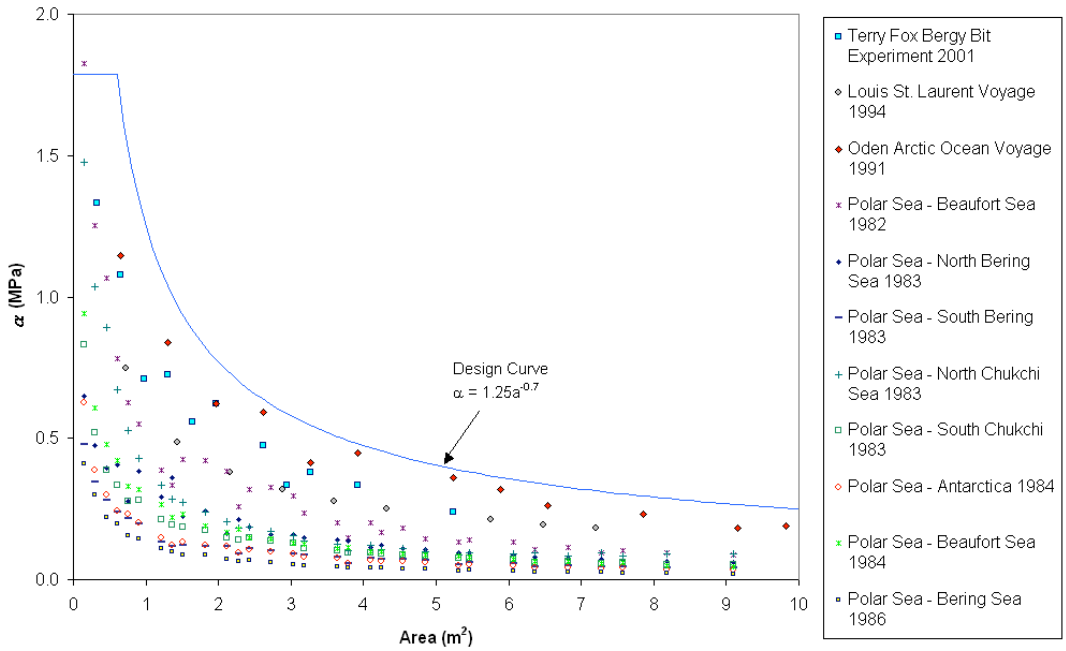

Figure 2. α versus area for ship-interaction data analysed by Taylor et al. (2009)

Full-scale ice pressure distributions

Data from the Japan Ocean Industries Association (JOIA) field indentation test program have been used to model the spatial load distributions corresponding to the time series ice crushing data for thin first-year sea ice. The program was carried out in Notoro Lagoon in Japan (1996-2000) and consisted of over thirty tests. Average ice thickness was on the order of 30 cm.

Additional details on the ice conditions, as well as physical properties of the ice may be found in Takeuchi et al. (1997) and Kaimo et al. (2000).

Erceg et al. (2014) analysed a dataset that corresponds to the event with ice thickness of 28.7 cm, a constant indentation rate of 0.3 cm/s, and duration of 73 s. From the tactile pressure sensor data for this event (950.4 mm wide by 237.6 mm high, with sensor element resolution of 5.1994 mm by 5.1994 mm), linear patterns of *hpz*s or "line-loads" were observed across the width of the interaction area; see Figure 4. Similar types of pressure distributions have been reported for ship-ice interactions (Riska, 1991) and other ice indentation events (Sodhi et al., 2001; Frederking, 2004; Taylor et al., 2008). The described ice crushing time history is used as a basis in the present analysis.

In order to investigate the effects of spatial variations in the pressure over design area, Erceg et al. (2014) identified pressure distributions with potentially high influence of *hpz*s using force to area logic, i.e. distributions with the highest ratio of total force and active area, see Figure 3. Herein, selected cases were scaled to introduce the equal amount of energy into the structure as for the uniform rule-based case so as to compare the response of the panel using the two design approaches. A cut off-limit of 80 MPa (dark red colour in Figure 5) was imposed on the scaled *hpz* pressure values to reflect the upper bound of expected maximum local ice pressures based on field data (Glen and Blount, 1984; Frederking et al., 1990; Masterson et al., 1993). The present paper utilizes only the pressure distribution with the highest calculated response, i.e. Case 1. The pressure patch is shown in Figure 5a. The total patch area corresponds to the area of tactile pressure sensors, while vertical boundaries, horizontal boundaries and dashed lines represent webframes, stringers and stiffeners of the stiffened panel, respectively.

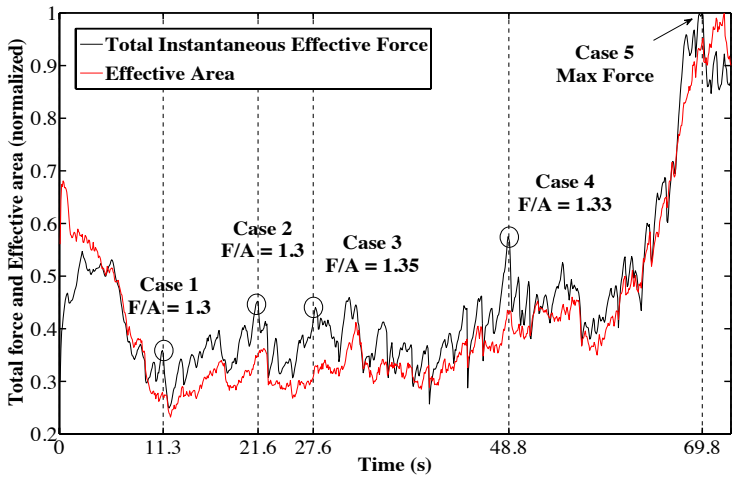

Figure 3. Time series of the measured force and effective area (Erceg et al., 2014).

CASE STUDY

Stiffened panel

In order to calculate the design pressures and the structural response, Erceg et al. (2015) used the hull lines of the product tanker MT Varzuga, built in 1976 as MT Uikku to ice class IAS of the FSICR. They modelled a stiffened panel parametrically in ANSYS Parametric Design Language to represent a part of the bow structure within the ice belt region under influence of ice loads. Structural configuration of the bow of MT Varzuga, as found in Vuorio (1998), was

simplified to a transversely framed 9-strake panel with two web frames with spacing S_{wf} = 2800 mm, two ice stringers with spacing S_{is} = 2350 mm, and stiffener spacing, s = 350 mm. The resulting scantlings are shown in Table 2 and the illustration of a 9-strake stiffened panel is shown in Figure 4.

Table 1. Scantlings of the panel according to IAS of the FSICR.

Plate thickness	20 mm
Webframe type	T800x360x18x26
Ice stringer type	T800x360x22x30
Stiffener type	HP240x11

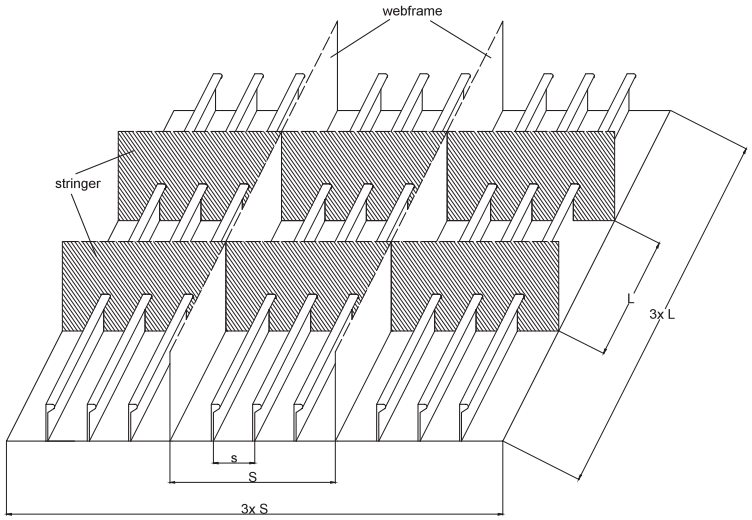

Figure 4. Illustration of a 9-strake stiffened panel dimensioned according to the FSICR. The pressure patches shown in Figure 1 are applied on the centre strake.

Ice loading calculation

Pressure patch size of 0.98 m^2 was chosen for the response comparison of the three methods as it resembles the shape of a typical ice-induced load on the ship hull. Height of the patch was defined by the class factor (350 mm for IAS), which combined with the span of stringer (i.e. webframe spacing S_{wf} = 2800 mm) gives the design area; see Figure 1 and Table 3. The obtained design pressure according to the FSICR was calculated to be 1.514 MPa; see Erceg et al. (2015).

For the same design area of 0.98 m^2, using the probabilistic method based on the example route from Kara Sea to the Bering Strait (8 transects on a 4500 km route), Erceg et al. (2015) obtained the design pressure of 5.025 MPa. The design curve $\alpha = 0.28A^{-0.7}$ for the North Bering Sea 1983 dataset was used for the calculations; see Figure 2. Ice conditions during the measurements (ice thickness ranging from 0.15 to 1.2 m) were in correspondence to the ones expected along the Northern Sea Route. The sailing window was chosen to be 4 months, out of which 2 were ice-free. Average speed of the ship was 7 knots.

Pressure distribution from Case 1 is applied to the structure used in Erceg et al. (2015) to compare the response using different approaches to account for ice loading. In order to do so, pressure distribution, Figure 5, is geometrically scaled to fit the new pressure patch size, as defined by the structural configuration of MT Varzuga (from S_{wf} = 950.4 mm to 2800 mm) and loading height (from s = 237.6 mm to 350 mm). First, the pressure distribution is scaled

to both horizontal and vertical (thickness) axes until the thickness of 350 mm is reached, which makes it 1400 mm wide. In the next step, the patch is mirrored horizontally to obtain a single pressure distribution with dimensions corresponding to MT Varzuga (350 mm by 2800 mm). By using this scaling approach, the aspect ratio of the pressure distribution is preserved. Also, by mirroring it, a symmetric load is obtained which features the characteristic phenomena of ice loads – line-like load and *hpz*s.

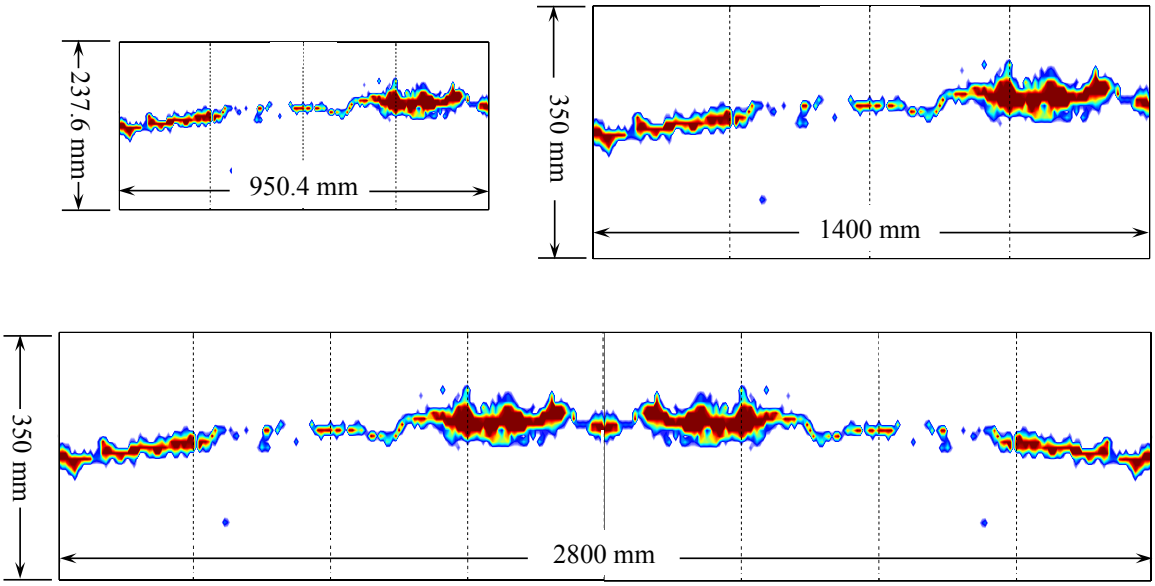

Figure 5. Procedure of scaling the pressure distribution to fit the structural configuration of MT Varzuga. Horizontal and vertical boundaries represent ice stringers and webframes, while dashed lines represent stiffeners in the centre strake.

Finally, in order to compare the panel response using the three approaches, the magnitude of pressure in the selected case is scaled to introduce the equal total amount of energy (i.e. total force over design area) into the structure as obtained using the rule-based method and probabilistic method, namely the design pressures of 1.514 MPa and 5.025 MPa, respectively. In both cases, a cut-off limit of 80 MPa is imposed on the scaled *hpz*s.

STRENGTH ASSESSMENT

The explicit nonlinear FEM solver LS-DYNA, version 971, is used for simulations. A bilinear material behaviour is implemented using material 3 of LS-DYNA; Table 3. Moreover, Hughes-Liu beams are used for modelling the HP flanges, and four nodded Belytschko-Lin-Tsay shell elements with five integration points for the remainder of the panel; see LS-DYNA Manual (2007) for element technology details. Small element size (8 mm) on the pressure patch is used to fully catch the pressure distribution. Mesh gets coarser further away from the patch, with 50 mm size of the elements near the edges of the panel. The 9-strake structure is clamped along both longitudinal and transversal edges as shown in Figure 1. As a result, webframes and stringers surround the centre strake, thus resembling realistic boundary conditions for this panel. The applied load history is modelled to represent a simplification one loading cycle of saw-tooth load observed in ice load measurements; see e.g. Frederking et al. (1990). Loads are set to increase linearly from zero at start to their full values at 0.01 s, remaining constant until 0.1 s, and then decreasing linearly to zero at 0.2 s. Termination time is set to be 0.3 s.

Table 2. Plastic kinematic material properties

Density	7850 kg/m3
Young's modulus	210 GPa
Yield strength	315 MPa
Tangent modulus	1.14 GPa

RESULTS

This paper extends the work by Erceg et al. (2015) who used the probabilistic approach based on measured data and expected exposure to select an appropriate ice class for a vessel navigating along the NSR and compared the results to the FSICR requirements. Their work was used as a basis for the response calculations conducted in this paper, including the case study structure from Figure 4 and loading cases from Figure 1. The obtained design pressures are shown in Table 3.

Table 3. Load lengths, corresponding design ice pressures and areas for transverse framing (Erceg et al., 2015)

Structure	l_a [m]	p_{FSICR} [MPa]	p_{PROB} [MPa]	Design area [m^2]
Shell *LC 2-4*	Frame spacing	3.271	19.2	0.123
Frames *LC 2-4*	Frame spacing	3.271	19.2	0.123
Stringer *LC 1*	Span of stringer	1.514	5.025	0.98
Webframe *LC 5*	2xWF spacing	1.145	3.146	1.96

The FSICR design load

In accordance with the requirements of the FSICR, Erceg et al. (2015) applied the load patch at locations where the capacity of the structure under combined effects of bending and shear is minimized. The highest von Mises stresses of 250 MPa were reported on the unsupported part of the plate, while stresses in other structural elements were significantly lower. No plastic deformation occurred in any of the analysed cases, which is in accordance with the FSICR requirements.

Probabilistic design method

For the chosen example route, ice conditions and exposure parameters, three design pressures were obtained, each corresponding to one design area; see Figure 1. Expectedly, the highest stress levels were measured in LC 2-4, where the design pressure patch had an area of only 0.123 m^2 and was primarily used to define the scantlings of the plate and framing; see Table 4. Those highly localized loads, resembling *hpz*s behaviour, cause plastic deformation on the plate and surrounding frames and webframes.

Table 4. Response of the structure to probabilistic design load for selected load cases (Erceg et al., 2015)

Load case	von Mises stress [MPa]				Pl. strain [e-2]	Resultant displacement [mm]
	Plate	Frames	WF	Stringers		
1a	315	240	197	178	0	≈0
2a	378	317	330	175	7.37	31
3b	393	313	85	250	8.24	25
5c	166	163	160	166	0	≈0

Full-scale ice pressure distribution

The magnitudes of pressure in the distribution from Figure 4 are first scaled to introduce the equal amount of energy into the structure as in the probabilistic design load approach, i.e. average pressure of 5.025 MPa over the area of 0.98 m^2. Due to the influence of *hpz*s, stress levels on the shell plating exceed 500 MPa (LC 1a, 1b), while stresses on frames and webframes also exceed the yield point; see Figure 4. Table 5 shows the overview of the results for the loading case with the highest response.

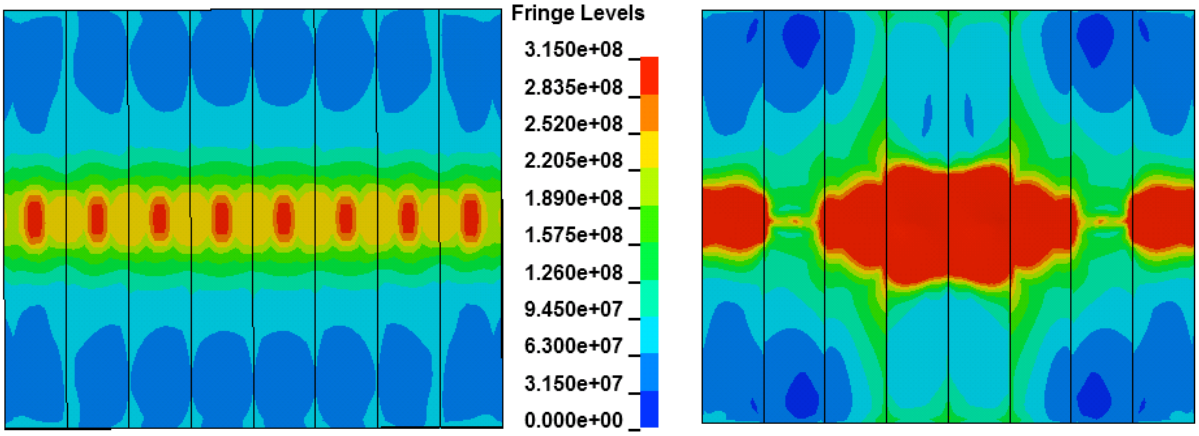

Figure 5. von Mises stress levels [Pa] on the centre strake for probabilistic design method and full-scale ice pressure distribution: LC 1a – load applied mid-height; p_{avg}=5.025 MPa

Table 5. Results overview – Probabilistic method vs. full-scale distribution

		Probabilistic method	Full-scale distribution
von Mises stress [MPa]	Plate	393	505
	Webframe	330	315
	Frame	315	360
	Ice stringer	250	205
Resultant displacement [mm]		31	22

Then, the pressure distribution is scaled to introduce the equal amount of energy as the FSICR design load, i.e. average pressure of 1.514 MPa over the area of 0.98 m^2. The results overview for the case with the highest response, LC 1b, is given in Table 6. Yield limit is reached on the unsupported part of the plate, while the stresses in the remaining elements fall well below the design limit. It is also interesting to observe that the stress level in ice stringers is higher for the FSICR method, as their requirements check the response to various design area sizes; see Figure 1.

Table 6. Results overview – The FSICR method vs. full-scale distribution

		FSICR method	Full-scale distribution
von Mises stress [MPa]	Plate	250	317
	Webframe	130	135
	Frame	130	235
	Ice stringer	65	60
Resultant displacement [mm]		5.1	7

In addition, the chosen pressure distribution is applied only as a quasi-static load of shape shown in Figure 4, thus not capturing the dynamic effects of ice loads observed in the nature.

DISCUSSION AND CONCLUSION

This paper wraps up the findings from Erceg et al. (2014, 2015) and indicates the need for an alternative to the rule-based ice load application model, which was already proposed in Kujala and Ehlers (2013, 2014) and Ehlers et al. (2014).

The response of a stiffened panel in the ice belt region was compared using different approaches to account for ice loading. The design pressures of the FSICR method and probabilistic method were utilized to create a full-scale pressure distribution with the equal amount of energy introduced onto the structure. For that purpose, pressure distribution from JOIA field indentation programme used in Erceg et al. (2014) was scaled in compliance with the FSICR requirements to represent a pressure patch on the hull of MT Varzuga. The FSICR defines the size of a pressure patch with load height (class factor) and load length, l_a. In the current analysis, l_a is taken to be one webframe spacing, thus simulating the ice impact on a 350 mm high by 2800 mm wide design area. The analysis of full-scale pressure distribution was conducted for three different load cases (LC 1a, 1b and 1c) from Figure 1 and compared the maximum stress values (LC 1-4) using both probabilistic and the FSCIR approach.

The results using full-scale ice pressure distributions show higher response by means of von Mises stress compared to both probabilistic and the FSICR approach; see Table 5 and 6. A comparison of stress distributions for uniform load and full-scale pressure distribution can be seen in Figure 5, with latter being highly localized as a consequence of *hpz*s acting on the structure. Yield point is reached when using probabilistic design load, both with uniform and full-scale pressure distribution, followed by plastic deformation on the structure. For the FSICR load, non-uniform load reaches the yield point in the unsupported part of the plate, but no plastic deformation is observed.

The influence of *hpz*s and line like load in full-scale distribution approach causes higher stress levels on the structure when compared to the approaches using uniform pressure patches, as the majority of the pressure is exerted through highly localized areas. Furthermore, different ice loading applications trigger different failure mechanisms – full-scale approach causes the highest response on the mid-plate and frames, while uniform load show relatively higher response on webframes and stringers. This paper further backs the work of Erceg et al. (2014, 2015), which indicated the need to consider the effects of spatial load distributions in design.

For the current analysis, a case study structure was used along the chosen pressure distribution from JOIA data, which was additionally scaled up and mirrored to comply with the requirements in the FSICR. Therefore, further work is needed to define a generally applicable case, including multiple structures, pressure distributions corresponding to different ice conditions and a study on the influence of dynamic variations found in ice. These will have to be explored in greater detail to assess which scenarios are the most representative of the conditions a vessel is likely to experience of its design lifetime. Nevertheless, the basic concept presented in this paper clearly indicates the changes in response due to spatial variations found in ice loads.

ACKNOWLEDGEMENTS
The financial support of MAROFF Competence building project funded by the Research Council of Norway on "Holistic risk-based design for sustainable arctic sea transport" is greatly acknowledged here.

REFERENCES
Ehlers, S., Erceg, B., Jordaan, I., Taylor, R., 2015. Structural analysis under ice loads for ships operating in Arctic waters. Proceedings of MARTECH 2014, 2nd International Conference on Maritime Technology and Engineering, Lisbon, Portugal, 15-17 October 2014.

Erceg, B., Taylor, R., Ehlers, S., Leira, B.J., 2014. A response comparison of a stiffened panel subjected to rule-based and measured ice loads. Proceeding of the 33rd International Conference on Ocean, Offshore and Arctic Engineering, Volume 10: Polar and Arctic Science and Technology. San Francisco, California, USA, June 8-13, 2014.

Erceg, B., Taylor, R., Ehlers, S., Leira, B.J., 2015. A response comparison of a stiffened panel subjected to rule-based and measured ice loads. Submitted to the 34th International Conference on Ocean, Offshore and Arctic Engineering (OMAE 2015).

Frederking, R.M.W., 2004. Ice pressure variations during indentation. Proceedings of the 17th IAHR International Symposium on Ice. 2004. Vol. 2. p. 307.

Frederking, R.M.W., Jordaan, I.J., McCallum, J.S., 1990. Field tests of ice indentation at medium scale: Hobson's Choice ice island 1989. Proceedings of 10th International Symposium on Ice, IAHR, Espoo, Finland, Vol. 2, pp. 931-944.

Glen, I.F., Blount, H., 1984. Measurements of ice impact pressures and loads onboard CCGS Louis S. St. Laurent. In Proceedings of the 3rd Offshore Mechanics and Arctic Engineering Symposium, vol. III. ASME, New Orleans, LA, 1984. p. 246-252.

Hallquist, J.O. 2007. LS-DYNA. Keyword User's Manual, Version 971, Livermore Software Technology Corporation.

Livermore Software Technology Corporation. LS-DYNA Keyword User's Manual. Vol I, May 2007.

Jordaan, I.J., 2001. Mechanics of ice-structure interaction. Engeering Fracture Mechanics, Vol. 68, pp. 1923-1968.

Jordaan, I.J., Maes, M.A., Brown, P.W., and Hermans, I.P., 1993. Probabilistic analysis of local ice pressures. Proceedings, 11th International Conference on Offshore Mechanics and Arctic Engineering, Calgary, AB, Vol. II, pp. 7-13.

Kaimo, Z., Takawaki, T., Matsushita, H., 2000. Medium scale field indentation tests: physical characteristics of first-year sea ice at Notoro Lagoon, Hokkaido. Proceedings of the Tenth International Offshore and Polar Engineering Conference. p. 562.

Kujala, P., 1991. Damage statistics of ice-strengthened ships in the Baltic Sea 1984-1987. Winter Navigation Research Board. Report. No. 50. 61 p. + app. 5 p.

Kujala, P., Ehlers, S., 2013. Limit state identification for ice-strengthened hull structures using measured long-term loads. Proceedings of the International Conference on Port and Ocean Engineering under Arctic Conditions (POAC'13).

Kujala, P., Ehlers, S., 2014. A risk-based evaluation ice-strengthened hull structures. ICETECH 2014.

Masterson, D.M., Frederking, R.M.W., Jordaan I.J., Spencer, P.A., 1993. Description of multiyear ice indentation tests at Hobson's Choice ice island - 1990. Proceedings of 12th International Conference on Offshore and Arctic Engineering. Vol. 4. Glasgow. pp. 145-55.

Ralph, F., Jordaan I.J., 2013. Probabilistic methodology for design of arctic ships. Proceedings of 32nd International Conference on Ocean, Offshore and Arctic Engineering (OMAE 2013), Vol. 6, Nantes, France, June 9-14, 2013.

Richard, M., Taylor, R., 2014. Analysis of High Pressure Zone Attributes from Tactile Pressure Sensor Field Data. Proceedings of the 33rd International Conference on Ocean, Offshore and Arctic Engineering, Vol. 10: Polar and Arctic Science and Technology, San Francisco, California, USA, June 8–13, 2014.

Riska, K., 1991. Observations of the Line-like Nature of Ship-Ice Contact. 11th International Conference on Port and Ocean Engineering under Arctic Conditions, Proceedings, Vol 2, St. John's, Canada, September 24-28, 1991, pp. 785 - 811.

Riska, K., Kämäräinen, J., 2011. A Review of Ice Loading and the Evolution of the Finnish-Swedish Ice Class Rules. Proceedings of the SNAME Annual Meeting and Expo. November 16-18, Houston (TX), USA.

Sodhi, D.S., Takeuchi, T., Kawamura, M., Nakazawa, N., Akagawa, S., 2001. Measurement of ice forces and interfacial pressures during medium-scale indentation tests in Japan. Proceedings of the International Conference on Port and Ocean Engineering under Arctic Conditions (POAC'01) p. 617.

Taylor, R., Jordaan, I., Li, C., Sudom, D., 2009. Local design pressures for structures in ice: analysis of full-scale data. Proceedings of the 28th International Conference on Ocean, Offshore and Arctic Engineering (OMAE 2009), May 31-June 5, Honolulu, Hawaii, USA.

Taylor, R., Richard, M., 2014. Development of a Probabilistic Ice Load Model based on Empirical Descriptions of High Pressure Zone Attributes. Proceedings of the 33rd International Conference on Ocean, Offshore and Arctic Engineering, Vol. 10: Polar and Arctic Science and Technology, San Francisco, California, USA, June 8–13, 2014.

Taylor, R.S., Frederking, R.F., Jordaan, I.J., 2008. The nature of high pressure zones in compressive ice failure. Proceedings of the 19th IAHR International Symposium on Ice, Vancouver.

Trafi, 2010. Ice Class Regulations 2010: "Finnish-Swedish Ice Class Rules 2010". Finnish Transport Safety Agency, 23.11.2010 TRAFI/31298/03.04.01/2010, 48 p.

Vuorio, J., 1998. Instrumentation of MT Uikku for ice load measurements. VTT research report. VAL37-980525, Espoo. (In Finnish)